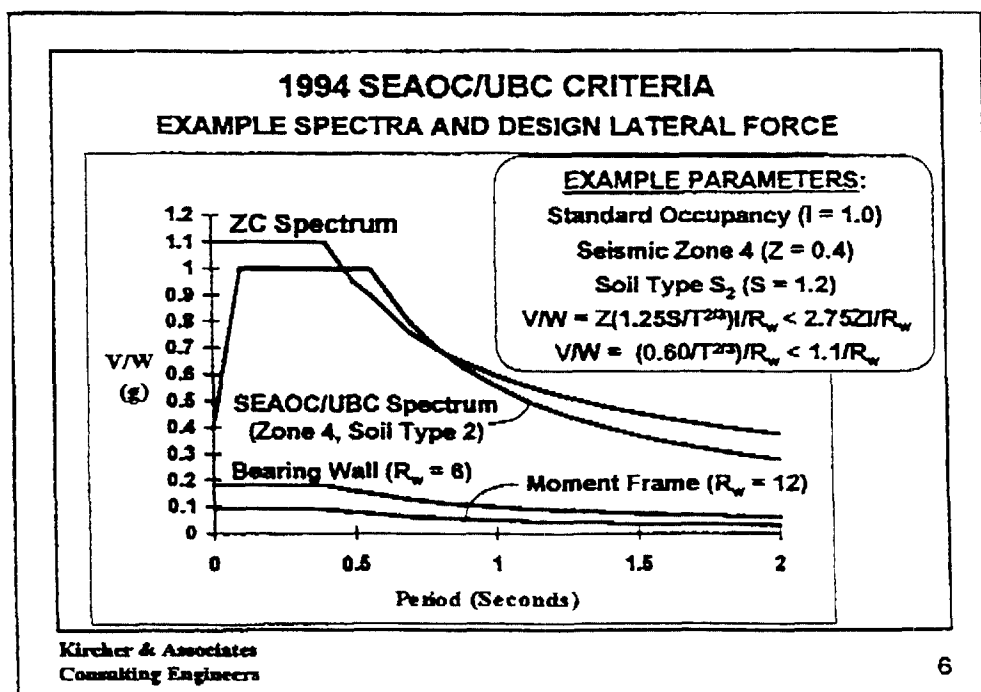
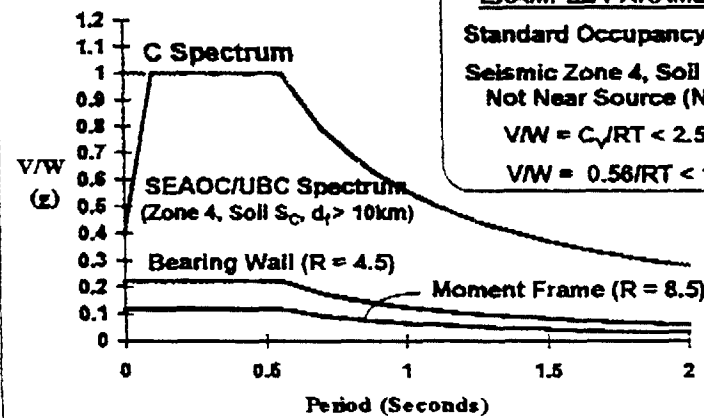


5



6

# **1997 SEAOC/UBC Criteria** **EXAMPLE SPECTRA AND DESIGN LATERAL FORCE**



## **EXAMPLE PARAMETERS:**

Standard Occupancy ( $I = 1.0$ )

Seismic Zone 4, Soil Type  $S_C$

Not Near Source ( $N = 1.0$ )

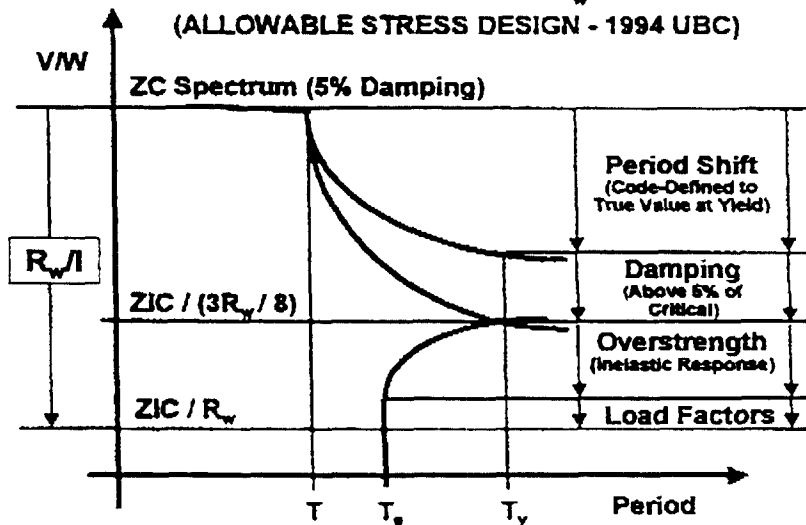
$$V/W = C_v/RT < 2.5C_A/R$$

$$V/W = 0.56/RT < 1.0/R$$

Kircher & Associates  
 Consulting Engineers

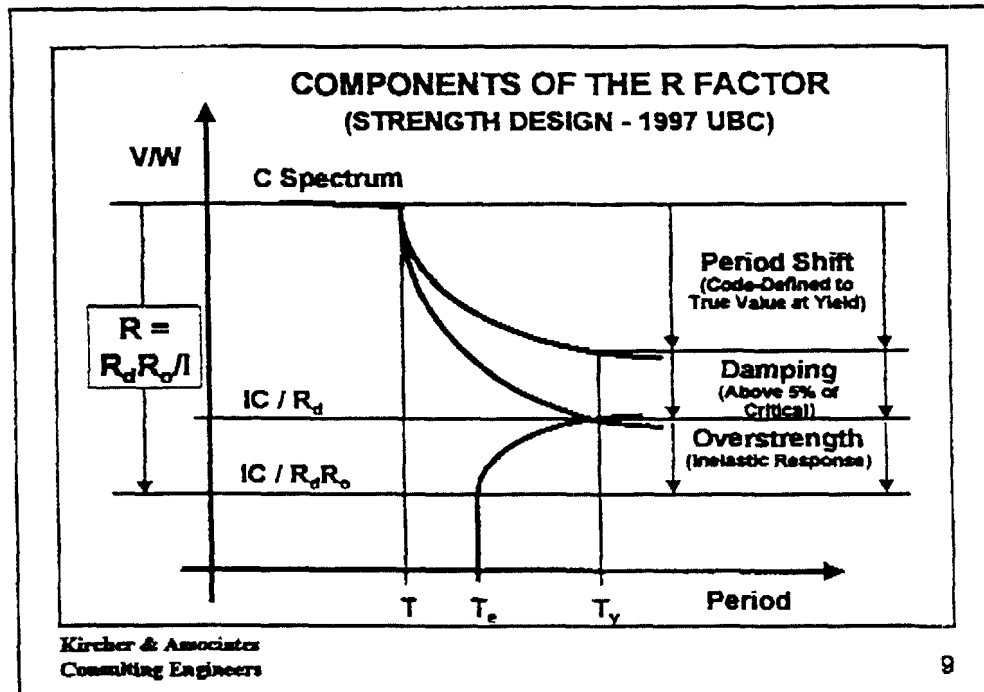
7

# **COMPONENTS OF THE $R_w$ FACTOR** **(ALLOWABLE STRESS DESIGN - 1994 UBC)**



Kircher & Associates  
 Consulting Engineers

8

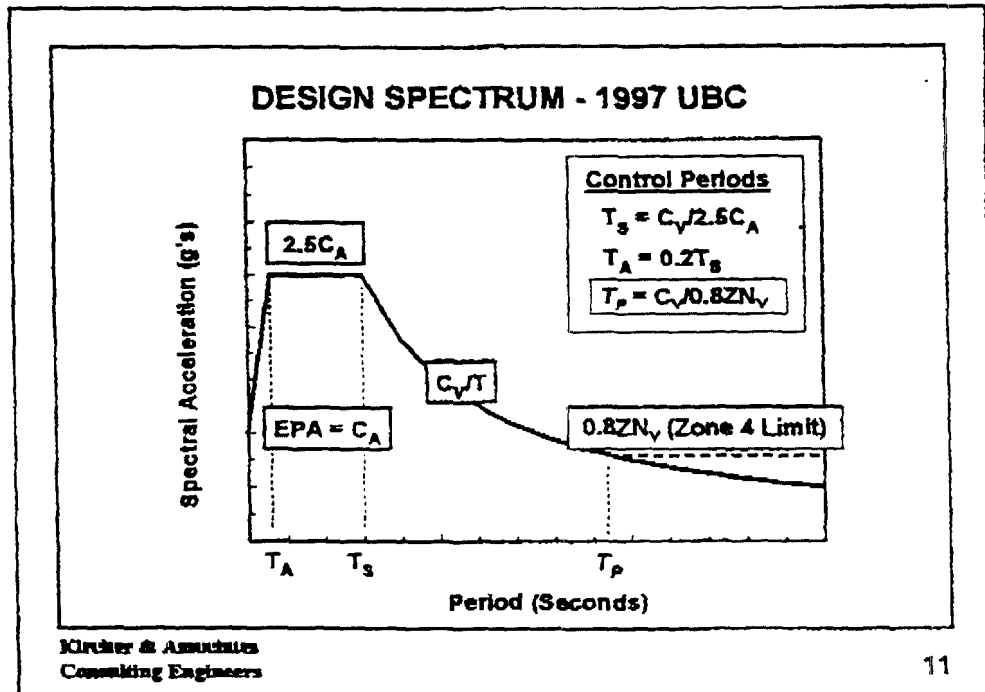


**SOIL PROFILE TYPES - 1997 UBC (NEHRP)**

Soil Profile Type	Soil Profile Name/Generic Description	Shear Wave Velocity (m/sec.)	Approx. 1994 UBC Soil Type
S <sub>A</sub>	Hard Rock (EUS Only)	> 1,500	S1
S <sub>B</sub>	Rock	760 to 1,500	
S <sub>C</sub>	Very Dense Soil and Soft Rock	360 to 760	S2
S <sub>D</sub>	Stiff Soil	180 to 360	
S <sub>E</sub>	Soft Soil	< 180	S3
S <sub>F</sub>	Soil Requiring Site-Specific Evaluation		S4

**Kircher & Associates**  
Consulting Engineers

10



11

**SHORT-PERIOD SEISMIC COEFFICIENTS - 1997 UBC**

- Short-Period (Acceleration-Domain) Relationship:

$$V = \frac{2.5 C_A}{(R/I)} W$$

- Values of Seismic Coefficients, C<sub>A</sub> (Table 16-Q):

Soil Type	Seismic Zone Factor, Z				
	Z=0.075 <sup>1</sup>	Z=0.15 <sup>1</sup>	Z=0.2 <sup>1</sup>	Z=0.3 <sup>1</sup>	Z=0.4 <sup>1</sup>
S <sub>A</sub>	0.06	0.12	0.16	0.24	0.32N <sub>A</sub>
S <sub>B</sub>	0.08	0.15	0.20	0.30	0.40N <sub>A</sub>
S <sub>C</sub>	0.09	0.18	0.24	0.33	0.40N <sub>A</sub>
S <sub>D</sub>	0.12	0.22	0.28	0.36	0.44N <sub>A</sub>
S <sub>E</sub>	0.19	0.30	0.34	0.36	0.36N <sub>A</sub>

Kircher & Associates  
Consulting Engineers

12

### LONG-PERIOD SEISMIC COEFFICIENTS - 1997 UBC

- Long-Period (Velocity-Domain) Relationship:

$$V = \frac{C_v}{(R/I)T} W \geq 0.11C_A I W \geq \frac{0.8Z N_v}{(R/I)} W \quad (\text{Zone } 4)$$

Values of Seismic Coefficient,  $C_v$  (Table 16-R):

Soil Type	Seismic Zone Factor, Z				
	Z=0.075 <sup>1</sup>	Z=0.15 <sup>1</sup>	Z=0.2 <sup>1</sup>	Z=0.3 <sup>1</sup>	Z=0.4 <sup>1</sup>
S <sub>A</sub>	0.06	0.12	0.16	0.24	0.32N <sub>v</sub>
S <sub>B</sub>	0.08	0.15	0.20	0.30	0.40N <sub>v</sub>
S <sub>C</sub>	0.13	0.25	0.32	0.45	0.56N <sub>v</sub>
S <sub>D</sub>	0.18	0.32	0.40	0.54	0.64N <sub>v</sub>
S <sub>E</sub>	0.26	0.50	0.64	0.84	0.96N <sub>v</sub>

Kircher & Associates  
Consulting Engineers

13

### NEAR SOURCE FACTOR $N_A$ - 1997 UBC

- Values of Near Source Factor,  $N_A$  (Table 16-S):

Seismic Source Type	Closest Distance to Known Seismic Source		
	≤ 2 km	5 km	≥ 10 km
A	1.5	1.2	1.0
B	1.3	1.0	1.0
C	1.0	1.0	1.0

- Seismic Source Type (Table 16-T):

Seismic Source Type	Seismic Source Description	Source Definition	
		Magnitude	Slip Rate
A	Large M & High Slip Rate	M ≥ 7.0	≥ 5 mm/yr
B	Not A or C Source		
C	No Large M & Low Slip Rate	M ≤ 6.5	≤ 2 mm/yr

Kircher & Associates  
Consulting Engineers

14

### NEAR SOURCE FACTOR $N_v$ - 1997 UBC

- Values of Near Source Factor,  $N_v$  (Table 16-T):

Seismic Source Type	Closest Distance to Known Seismic Source			
	$\leq 2$ km	5 km	10 km	$\geq 15$ km
A	2.0	1.6	1.2	1.0
B	1.6	1.2	1.0	1.0
C	1.0	1.0	1.0	1.0

- Seismic Source Type (Table 16-U):

Seismic Source Type	Seismic Source Description	Source Definition	
		Magnitude	Slip Rate
A	Large M & High Slip Rate	$M \geq 7.0$	$\geq 5$ mm/yr
B	Not A or C Source		
C	No Large M & Low Slip Rate	$M \leq 6.5$	$\leq 2$ mm/yr

Kircher & Associates  
Consulting Engineers

15

### BASIS FOR NEAR SOURCE FACTOR

- Near-source factors developed by the Ground Motion Subcommittee of the SEAOC Seismology Committee as an extension of the N factor required for base-isolated buildings
- Near-source factors are based on the increase in ground shaking, above Zone 4 level, predicted by empirically-derived median estimates of ground motion for:
  - moment magnitude  $M = 7.5$  - Type A faults
  - moment magnitude  $M = 7.0$  - Type B faults
- Median estimates of ground motion based on the average of Boore, Joyner, Fumal (BJF 93/94) and Sadigh, Chang, Abrahamson, Chiou, Power (Sadigh 93) attenuation functions
- Same combination of attenuation functions used by Project '97 (USGS) to develop the new spectral maps of the 1997 NEHRP Provisions for rock/stiff soil sites in the western US:
  - $1/4\text{BJF } 93/94(\text{A}) + 1/4\text{BJF } 93/94(\text{B}) + 1/2\text{Sadigh '93 (Rock)}$

Kircher & Associates  
Consulting Engineers

16

### BASIS FOR NEAR SOURCE FACTOR

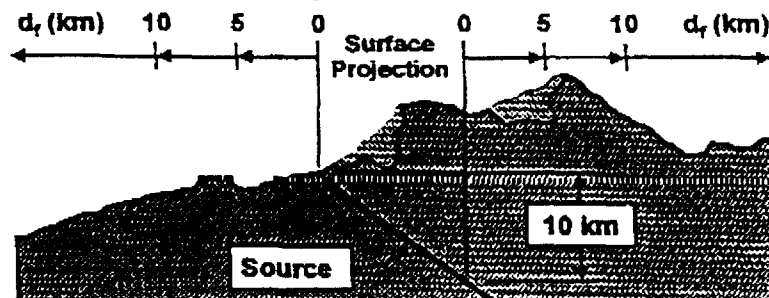
- Near-source factors apply to both strike-slip and reverse-slip (thrust) fault mechanisms (although reverse-slip faults produce about 20% greater shaking, on the average)
- Short-period (acceleration-domain) near-source factor ( $N_A$ ) based on response at 0.3 seconds and long-period (velocity-domain) near-source factor ( $N_V$ ) based on 1.0-second response
- Values of  $N_V$  are bumped upward by about 20% to account for the increase in average response in the fault-normal direction above that predicted by the attenuation functions for the random component of horizontal ground shaking (Somerville, 1996, 7th US/Japan Workshop, Lessons Learned from Kobe and Northridge).
- Commentary to SEAOC Blue Book notes that ground shaking at "forward directivity" sites is likely be about 1.25 times the  $C_V$  (and  $C_A$ ) coefficients based on average fault-normal response

Kircher & Associates  
Consulting Engineers

17

### DISTANCE TO SOURCE - 1997 UBC

- The "closest distance to known seismic source" ( $d_r$ ) shall be taken as the minimum distance between the site and the area described by the surface projection of the source. The surface projection need not include portions of the source at depths of 10 km, or greater.



Kircher & Associates  
Consulting Engineers

18

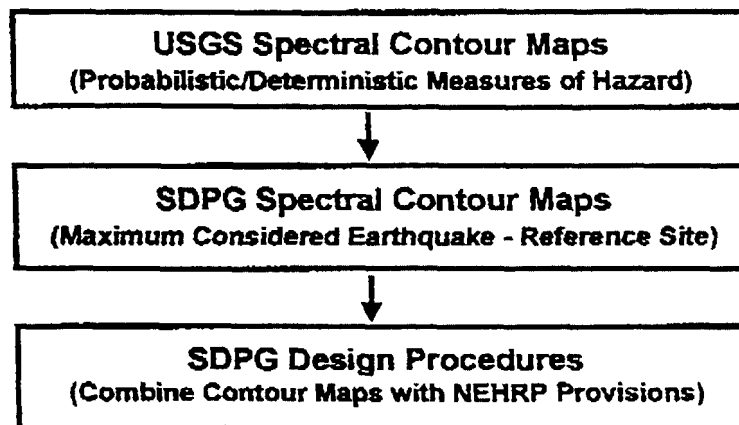
### PROJECT '97

- Joint Effort: BSSC, FEMA and USGS
- Purpose: Update *NEHRP Recommended Provisions for the development of Seismic Regulations for New Buildings*, including up-to-date seismic hazard maps and related design procedure
- Seismic Design Procedures Group (SDPG) Goals:
  - Replace existing effective peak ground acceleration and velocity design maps with spectral response design maps based on new USGS spectral response hazard maps
  - Develop and propose new design values maps that are consistent with the framework of the NEHRP Provisions
  - Develop and propose new design procedures for use with the new design values maps in the NEHRP Provisions

Kircher & Associates  
Consulting Engineers

19

### DEVELOPMENT OF SEISMIC INPUTS



Kircher & Associates  
Consulting Engineers

20

### NEW EARTHQUAKE DEFINITIONS ASSUMPTIONS AND TENTATIVE PROCEDURES

- For all Seismic Zones: Define consistent relationship between Design Earthquake (DE) and Maximum Considered Earthquake (MCE) shaking levels:

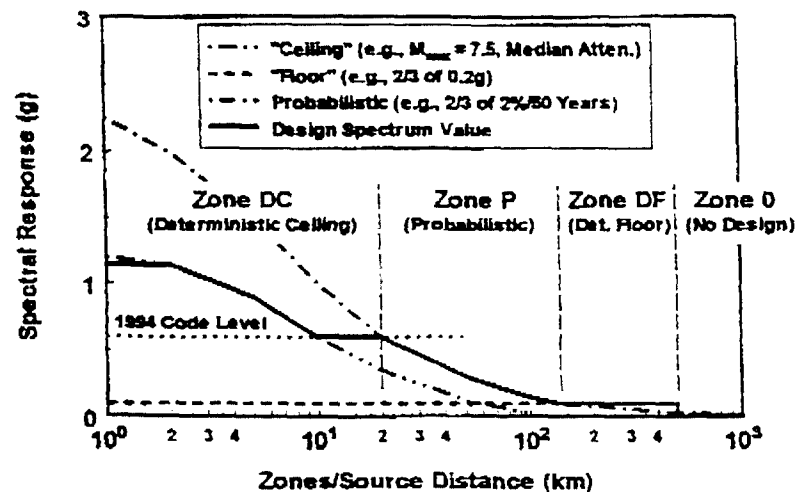
$$DE = \frac{2}{3} MCE \quad \text{or} \quad MCE = (1.5) DE$$

- DE is the "design-basis" earthquake, used for "regular" design, with margin provided by intentional conservatism's of the NEHRP Provisions
- MCE is the "worst-case/no collapse" earthquake, used for design of special (base isolated) buildings or for collapse check of existing buildings [FEMA 273]

Kircher & Associates  
Consulting Engineers

21

### DESIGN EARTHQUAKE CRITERIA

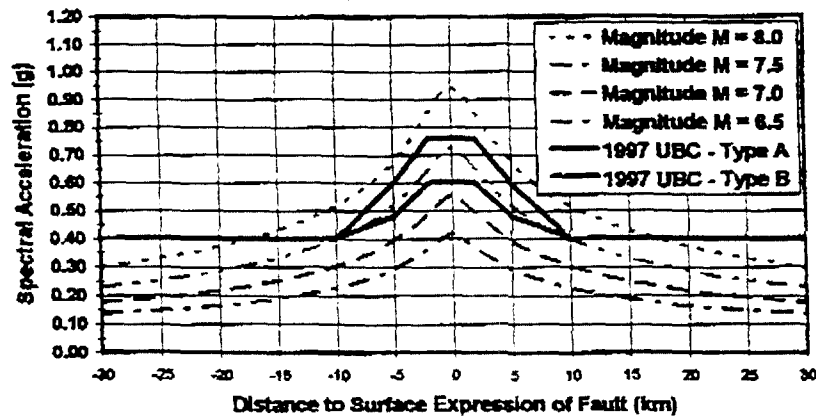


Kircher & Associates  
Consulting Engineers

22

### COMPARISON OF 1997 UBC & NEHRP PROVISIONS (1.0-SECOND RESPONSE NEAR STRIKE-SLIP FAULTS)

NEHRP =  $1/4BJF'93(A) + 1/4BJF'93(B) + 1/2Sadigh'93$   
Rock Sites, Strike-Slip Fault (Width = All, Dip = 0 Degrees)

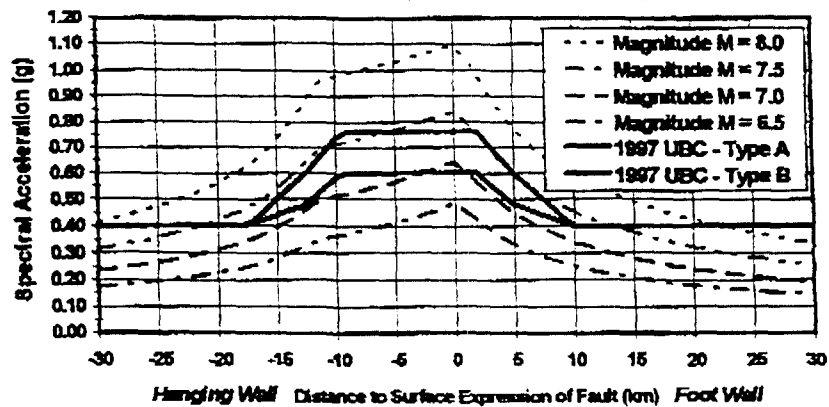


Kircher & Associates  
Consulting Engineers

23

### COMPARISON OF 1997 UBC & NEHRP PROVISIONS (1.0-SECOND RESPONSE NEAR THRUST FAULTS)

NEHRP =  $1/4BJF'93(A) + 1/4BJF'93(B) + Sadigh'93$   
Rock Sites, Thrust Fault (Width = 15 km, Dip = 450)



Kircher & Associates  
Consulting Engineers

24

## Near-Source Summary

- Earthquake ground shaking in the near-source region can be violent and capable of collapsing weak, non-ductile buildings, particularly if irregular in configuration.
  - Earthquake recordings near fault rupture indicate site response as much as twice that of 1994 UBC design spectra (Zone 4 sites).
- The 1997 UBC (1996 SEAOC "Blue Book") includes new near-source ( $N_A$  and  $N_V$ ) factors that substantially increase design base shear for buildings located near faults.
  - 1997 UBC near-source factors are similar to the near-fault factors required for design of base-isolated structures by the 1991 and 1994 UBC's (1990 SEAOC "Blue Book")
  - 1997 UBC near-source factors are required for design of all buildings, except short, stiff buildings of regular configuration.

Charles Kircher, Ph.D., P.E.  
SEAOC Seismology Committee

July 9, 1997 Near-Source Presentation  
California Seismic Safety Commission

### Supplementary Documents:

- (1) "The Kobe Earthquake: Ground Shaking, Damage and Loss," Charles A. Kircher, *Proceedings of Structures Congress XIV*, April 15 - 19, 1996, Chicago, Illinois, ASCE, New York, New York.  
*This paper describes near-source ground shaking and summarizes damage and loss statistics for buildings located within 5 km of fault rupture during the 1995 Kobe earthquake.*
- (2) "Ground Shaking Criteria: 1997 Codes and Beyond," (slide set), Charles A. Kircher and Robert E. Bachman, *SMIP97: Utilization of Strong-Motion Data*, May 8, 1997, California Division of Mines and Geology, Sacramento, California.  
*These slides describe and compare seismic ground shaking criteria of the 1994 UBC, 1997 UBC and the 1997 NEHRP Provisions (2000 IBC) with special emphasis on new site near-source factors of the 1997 UBC.*
- (3) January 22, 1996, Letter from Professor James M. Kelly, University of California at Berkeley, to Mr. David Choi of the California Office of Statewide Health Planning and Development.  
*This letter responds to an OSHPD request to review a paper by Hall, Heaton and others on the response of flexible buildings to near-source ground motion and raises concerns regarding methods used in the subject paper to model and evaluate base-isolated buildings.*

Seventh U.S.-Japan Workshop on Improvement of Structural Design and Construction Practices, Lessons Learned from Kobe and Northridge. Jan. 18-20, 1996, Kobe

## **FORWARD RUPTURE DIRECTIVITY IN THE KOBE AND NORTHRIDGE EARTHQUAKES, AND IMPLICATIONS FOR STRUCTURAL ENGINEERING**

by Paul Somerville

Woodward-Clyde Federal Services, 566 El Dorado Street, Pasadena, CA 91101

Tel: (818) 449-7650 Fax: (818) 449-3536 Email: pgsomer0@wcc.com

### **Abstract**

The ground motion characteristics of the Kobe and Northridge earthquakes were very similar, with each earthquake generating large near-fault motions due to forward rupture directivity effects. The largest recorded peak velocities in the two earthquakes were the same: 175 cm/sec in the fault-normal direction at Takatori, Kobe and Rinaldi, San Fernando. The effects of forward rupture directivity on near-fault ground motions are very similar for the 1995 Kobe, 1994 Northridge and 1989 Loma Prieta earthquakes, even though these earthquakes had different faulting mechanisms. Averaged over these three earthquakes, the absolute amplitudes of average horizontal ground motions containing forward directivity effects are 50% larger than those for average directivity conditions for magnitude 7 and closest distance 5 km for periods longer than about 0.5 second. Also, the ratio of fault normal to average horizontal ground motion for forward directivity is about twice as large as for average directivity conditions in this period range. New provisions in the proposed 1997 revision of the UBC for near-fault motions appear to provide an adequate representation of the average horizontal component for forward rupture directivity conditions, but are significantly lower than the fault normal component at periods longer than about 0.8 sec. Although both the Kobe and Northridge earthquakes occurred within dense urban regions, the damage estimate for the Kobe earthquake is about one order of magnitude larger than that for the Northridge earthquake. This large difference in damage may have been due in part to differences in the location of the region that experienced very large long-period ground motions produced by rupture directivity effects. In Kobe, the largest long period motions were within the densely populated urban regions, whereas for Northridge, the largest long period motions were to the north of the densely populated urban region. This suggests that losses of Kobe proportions could potentially occur during earthquakes in California if forward rupture directivity conditions occur within densely populated urban regions.

### **Introduction**

The rupture of the Kobe earthquake directly into downtown Kobe produced near-fault ground velocity time histories having large, brief pulses of ground motion. These long-period pulses are indicative of rupture directivity effects and are potentially damaging to multi-story buildings and other long-period structures such as bridges. Rupture models of the Kobe earthquake that explain these pulses have been derived by several investigators including Sekiguchi et al. (1995), Wald (1995), and Yoshida et al. (1995). Rupture directivity effects have also been widely observed in near fault strong motion data in California (Somerville and Graves, 1993), and their average effect has been quantified as a modification to empirical attenuation relations by Somerville et al. (1995).

Although the focus of this paper is on rupture directivity effects, they were not the only contributor to the large ground motions caused by the Kobe earthquake. Much of the damage from the Kobe earthquake was concentrated in a region where there is a shallow layer of alluvium. The zone of severe damage, which coincided with a layer of thin alluvium about 10 meters thick, lies to the southeast of the mapped active faults that are inferred to have ruptured at depth, indicating that the widespread damage in this zone is not explained simply by proximity to the fault rupture. Preliminary measurements of site response indicate large amplification of ground motions within this zone (Kawase et al., 1995). Similar conditions exist in many parts of California, such as Oakland and Long Beach. We do not have many recordings of large earthquakes on thin soil sites at close distances in the United States, which makes the Kobe data of special importance for evaluating the response of thin soils to strong shaking from large earthquakes in California.

### **Rupture Directivity Effects**

At long periods (longer than about 1 second), ground motions are strongly influenced by the earthquake faulting mechanism (the orientation of the fault and the direction of slip on the fault); the location of the earthquake hypocenter; and the location of the recording station in relation to the fault. A particularly important effect at long periods is the rupture directivity effect in near-fault strong ground motion, which is manifested by a large long-period pulse of motion in the direction normal to the fault.

Not all near-fault locations experience forward rupture directivity effects. The forward rupture directivity effect occurs when two conditions are met: the rupture front propagates toward the site, and the direction of slip on the fault is aligned with the site. The propagation of the rupture toward the site at a velocity that is almost as large as the shear wave velocity causes most of the seismic energy from the rupture to arrive in a single large pulse of motion which occurs at the beginning of the record. This pulse of motion represents the cumulative effect of almost all of the seismic radiation from the fault. The radiation pattern of the shear dislocation on the fault causes this large pulse of motion to be oriented in the direction perpendicular to the fault. Backward directivity effects, which occur when the rupture propagates away from the site, give rise to the opposite effect: long duration motions having low amplitudes at long periods.

### **Rupture Directivity Effects in Strong Motions Recorded during the 1995 Kobe earthquake**

The conditions for generating rupture directivity effects are readily met in strike-slip faulting, where the fault slip direction is oriented horizontally in the direction along the strike of the fault, and rupture propagates horizontally along strike either unilaterally or bilaterally. The rupture of the Kobe earthquake directly into downtown Kobe caused near-fault rupture directivity effects. The recorded peak velocities were as large as 175 cm/sec at Takatori in western Kobe, and the largest values occurred in the densely populated urban region, as shown in Figure 1. In Figure 2, we show the acceleration, velocity and displacement time histories of the Kobe earthquake recorded at Kobe JMA. The near-fault ground velocity time histories have large, brief pulses of ground motion that are indicative of rupture directivity effects. The horizontal peak velocity and displacement in the fault normal direction are about two and three times as large respectively as those in the fault parallel direction, but this difference diminishes at short periods

(peak acceleration). The acceleration response spectrum of the fault normal component greatly exceeds that of the fault parallel component for periods longer than 0.5 second, as seen in Figure 3.

### **Rupture Directivity Effects in Strong Motions Recorded during the 1995 Northridge event**

The conditions required for forward directivity are also met in dip slip faulting, including both reverse and normal faults. In this case, coincidence of the fault slip alignment and the rupture direction occurs in the updip direction, causing forward rupture directivity effects at sites located updip from the hypocenter. Unlike the case for strike-slip faulting, where we expect forward rupture directivity effects to be most concentrated away from the hypocenter, dip slip faulting produces directivity effects that are most concentrated updip from the hypocenter.

The rupture of the Northridge earthquake updip and toward the north produced near-fault rupture directivity effects along the northern margin of the San Fernando Valley (Wald and Heaton, 1994). The recorded peak velocities were as large as 175 cm/sec at Rinaldi in the northern San Fernando Valley, but unlike the Kobe earthquake, the largest values occurred outside the densely populated urban region, as shown in Figure 4. In Figure 5, we show the acceleration, velocity and displacement time histories of the Northridge earthquake recorded at Rinaldi. The near-fault ground velocity time histories have large, brief pulses of ground motion that are indicative of rupture directivity effects. The horizontal peak velocity and displacement in the fault normal direction are about twice as large as those in the fault parallel direction. The acceleration response spectrum of the fault normal component greatly exceeds that of the fault parallel component for periods longer than 0.5 second, as seen in Figure 6.

### **Average Rupture Directivity Effects**

Somerville et al. (1995) developed modifications to empirical attenuation relations to incorporate average rupture directivity conditions. The modifications, based on an empirical analysis of near-fault data and checked using broadband strong motion simulations, give the fault-normal and fault-parallel components of motion, which differ from each other at periods longer than one-half second in a manner that is both magnitude- and distance-dependent. The earthquakes used in the regression analysis of recorded data include all California crustal earthquakes with magnitudes of 6 or larger for which digital strong motion data and faulting mechanism are available (including the 1994 Northridge earthquake), together with selected crustal earthquakes from other regions (including the 1995 Kobe earthquake) to augment the data set for larger magnitudes. The data set provides a fairly uniform sampling of the magnitude range of 6.0 to 7.5 and the distance range of 0 to 50 km. The dependence of the ratio of fault-normal to average response spectral acceleration on magnitude, distance, style of faulting, and site category was examined by means of a regression analysis of the data using the random effects method (Abrahamson and Youngs, 1992). This method provides a means of partitioning random variability in ground motion amplitudes into inter-event and intra-event terms, and ensures that the results of the regression are not unduly influenced by events having large numbers of recordings. The style of faulting and site terms were found not to be significant.

The model of the fault-normal to average ratio is displayed in Figure 7, which shows the distance dependence of the fault-normal to average horizontal ratio for various magnitudes and periods at the top, and the period dependence of the ratio for various magnitudes and distances at the bottom. For periods longer than 0.5 seconds, the ratio increases as magnitude increases and as distance decreases. The largest ratios occur within about 10 km of the fault. Generally, the ratio increases with increasing period up to about 5 seconds, where it tends to level off for all but the closest distances and largest magnitudes. In Figure 8, we apply this model to calculate response spectra for a magnitude 7 earthquake recorded at a closest distance of 6 km on soil for average rupture directivity conditions. The fault normal and fault parallel spectra diverge at periods longer than 0.5 seconds.

### **Forward Rupture Directivity Effects**

The model shown in Figure 7 is appropriate for estimating the fault normal and fault parallel components of ground motion under average rupture directivity conditions, and can be used in either probabilistic or deterministic seismic hazard analyses. The deterministic approach, which is based on the occurrence of a maximum magnitude earthquake on the controlling source, will give the fault normal and fault parallel motions at a given site averaged over rupture directivity conditions. However, it may be desired to include the most severe rupture directivity condition (forward directivity) in the deterministic approach, since forward directivity has a high likelihood of occurring at any near-fault site. Accordingly, we have developed a second modification that allows the estimation of ground motions having forward rupture directivity effects. This was done by quantifying the difference between forward rupture directivity effects and average directivity effects. The difference is characterized by two factors: an increase in the level of average ground motions, and by an increase in the ratio of fault normal to average ground motions. These adjustment factors can be applied to the average horizontal ground motion derived from empirical attenuation relations.

### **Comparison of Forward Rupture Directivity Effects in the Kobe, Northridge, and Loma Prieta Earthquakes**

We quantified forward rupture directivity effects in the near-fault strong motion recordings of three recent earthquakes in the magnitude range of 6.7 to 7.0. These are the 1989 Loma Prieta earthquake (oblique faulting), the 1994 Northridge earthquake (reverse faulting), and the 1995 Kobe earthquake (strike-slip faulting). The recordings used in the analysis are listed in Table 1. The results of the analysis are shown in Figure 9. At the top, we show the ratio of fault normal to average ground motions, which is quite similar for all three earthquakes even though they have different rupture mechanisms. The ratio averaged over the three events, shown by the bold line, is about twice as large as for average rupture directivity conditions.

At the bottom of Figure 9, we show the ratio of the average horizontal motion from the forward directivity records to the motion predicted by the empirical attenuation relation of Abrahamson and Silva (1995). The ratio becomes larger than zero at periods longer than about 0.5 second. The average horizontal ground motion for forward rupture directivity conditions is about 50% larger than for average rupture directivity conditions. The period dependence of this ratio is similar to that of the ratio of fault normal to average horizontal ground motions. This

indicates that the large fault normal motion caused by forward rupture directivity effects causes the average horizontal motion for forward rupture directivity to exceed that for average rupture directivity conditions.

Table 1. Data used in analysis of forward rupture directivity effects

Earthquake	Magnitude (Mw)	Mechanism	Recording Stations
1989 Loma Prieta	7.0	oblique	Lexington Dam Los Gatos Saratoga
1994 Northridge	6.7	thrust	Newhall Olive View Rinaldi Sylmar converter stn
1995 Kobe	6.9	strike-slip	Kobe JMA Port Island Takatori

In Figure 10, we have estimated the ground motions for forward directivity conditions for a magnitude 7 strike-slip earthquake recorded at a closest distance of 6 km on soil. We first modified the average horizontal ground motion derived from the empirical attenuation relation of Abrahamson and Silva (1995) in order to represent the average of the two horizontal components for forward directivity conditions. The increase is about a factor of about 1.5 for periods longer than about 0.5 second. Based on this average component, we then estimated the fault normal and fault parallel motions for forward directivity conditions. These are a factor of about 1.5 higher and lower respectively than the average ground motions for forward directivity conditions for periods longer than about 0.5 second. The combination of these two modifications for forward directivity conditions results in the fault normal motion being about 2 times higher than the average given by the empirical attenuation relation for periods longer than about 0.5 second, and the fault parallel motion being about the same as the average given by the empirical attenuation relation.

#### **Adequacy of Current Design Approaches for Representing Forward Rupture Directivity Effects**

In Figure 10, we also compare the spectra derived above for forward rupture directivity conditions for a magnitude 7 strike-slip earthquake at 6 km with the spectrum from the proposed 1997 UBC for a distance of 5 km from a highly active fault. This spectrum matches the average horizontal component for forward rupture directivity quite well, but is significantly lower than the fault normal component at periods longer than about 0.8 sec. The spectral shape of the UBC

spectrum may need to be broadened to longer periods to accommodate fault-normal motions from forward rupture directivity.

Currently, buildings over 60 meters in height in the Kansai District in Japan are designed to withstand peak velocities of 40 cm/sec without collapse. The peak velocities recorded at Fukiai and Takatori were about 100 cm/sec and 175 cm/sec respectively, and it has been estimated by Kawase and Hayashi (1995) that the strong ground motions in the heavily damaged part of the Sannomiya district in Chuo Ward, Kobe exceeded 100 cm/sec. The fact that many modern structures probably experienced ground motions that substantially exceeded the current design levels without serious damage has important implications for the evaluation of structural analysis and design. Recent modeling analyses by Heaton et al. (1995) have suggested that modern buildings may collapse when subjected to very large near-fault ground motions. The performance of modern buildings in Kobe may provide a valuable experimental basis for assessing these analyses.

### **Engineering Implications of Forward Rupture Directivity Effects: Kobe, Northridge and Future Earthquakes**

#### ***The Kobe earthquake - a worst case scenario for long-period ground motions***

The Kobe earthquake was a magnitude Mw 6.9 strike-slip earthquake that ruptured directly into downtown Kobe, producing forward rupture directivity effects throughout Kobe and adjacent cities. The largest recorded peak velocities were in the densely populated urban region, as shown in Figure 1.

#### ***Worst case scenarios (like Kobe) for strike-slip earthquakes in California***

There are many densely populated urban regions in California which, like Kobe, are located very close to major strike-slip faults. These include San Diego (Rose Canyon fault); San Bernardino (San Andreas and San Jacinto faults); Long Beach and the Port of Los Angeles (Palos Verdes fault); Hollywood and West Los Angeles (Hollywood and Santa Monica faults); cities on the east San Francisco Bay (Hayward fault); and cities on the San Francisco Peninsula (San Andreas fault). However, California has not experienced a strike-slip earthquake that ruptured directly into a heavily populated urban region, and has no experience of a strike-slip earthquake rupturing into the downtown region of a major city since the 1933 Long Beach earthquake. We therefore do not have much data from California on the performance of structures exposed to rupture directivity effects from a strike-slip earthquake that ruptured directly into an urban region, as occurred in Kobe. The strong motion characteristics of the Kobe earthquake, including its near-fault rupture directivity effects, are comparable to those that have been recorded close to fifteen crustal earthquakes in California in the past 25 years. The performance of soils and structures during the Kobe earthquake may therefore be very useful for predicting damage effects from an urban strike-slip earthquake in California.

### ***The Northridge earthquake - a best case scenario for long-period ground motions in Los Angeles***

The 1994 Northridge earthquake occurred on a blind thrust fault beneath the San Fernando Valley. The earthquake ruptured updip to the north, away from the dense urban region, and produced large peak velocities in the northern San Fernando Valley and adjacent Santa Susana Mountains, as shown in Figure 4. Although the Northridge earthquake occurred beneath an urban region, almost all of the faulting occurred at depths greater than 10 km. The great majority of the multi-story buildings in the San Fernando Valley were at least 15 km from the closest part of the fault, and were not exposed to large peak velocities due to forward rupture directivity effects, because these buildings are mostly located along the southern margin of the valley. Considering this lack of exposure of the dense urban region to large long-period ground motions due to forward rupture directivity, the Northridge earthquake was a best-case scenario. With the exception of freeway bridges and a few large buildings in the northern San Fernando Valley and adjacent mountains, it did not provide us with data (of the kind available from Kobe) on the performance of structures exposed to rupture directivity effects.

### ***Worst case scenarios for thrust earthquakes in Los Angeles***

Recent studies have proposed the presence of blind thrust faults underlying many parts of the greater Los Angeles region (Dolan et al., 1995). Unlike the Northridge earthquake, which ruptured safely to the north away from the dense urban region, some of these blind thrust faults may rupture directly toward dense urban regions. These include the Elysian Park thrust, which could rupture toward downtown Los Angeles; the Santa Monica Mountains thrust, which could rupture toward Hollywood, West Los Angeles and Santa Monica; and the Compton thrust, which could rupture toward coastal cities between Santa Monica and Huntington Beach. These earthquakes would cause the largest long-period ground motions to occur within densely populated urban regions, as occurred in Kobe, instead away from the dense urban region, as occurred in Northridge (Somerville and Graves, 1995).

### **Conclusions**

The effects of forward rupture directivity on near-fault ground motions are very similar for the 1995 Kobe, 1994 Northridge and 1989 Loma Prieta earthquakes, even though these earthquakes had different faulting mechanisms. This indicates that for engineering purposes, it is not necessary to distinguish between different styles of faulting in characterizing near-fault rupture directivity effects. Averaged over these three earthquakes, the absolute amplitudes of average horizontal ground motions containing forward directivity effects are 50% larger than those for average directivity conditions for magnitude 7 and closest distance 5 km for periods longer than about 0.5 second. Also, the ratio of fault normal to average horizontal ground motion for forward directivity is about twice as large as for average directivity conditions in this period range. New provisions in the proposed 1997 revision of the UBC for near-fault motions appear to provide an adequate representation of the average horizontal component for forward rupture directivity conditions, but are significantly lower than the fault normal component at periods longer than about 0.8 sec.

Given the widespread damage that occurred in Kobe, and the similarity between the strong ground motions experienced there and those that have been recorded outside urban regions in California, it is important to make loss estimates for urban earthquakes in California based on the performance data from Kobe, and to assess whether they may greatly exceed those of the 1994 Northridge earthquake. If it is concluded that losses of Kobe proportions could occur in an urban earthquake in California, this could have important implications for code provisions and other policy decisions concerning the reduction of earthquake damage in the United States.

## References

- Abrahamson, N.A. and R. R. Youngs, "A stable algorithm for regression analyses using the random effects model," *Bull. Seism. Soc. Am.*, **82**, pp. 505-510 (1992).
- Abrahamson, N.A. and W.J. Silva (1995). A consistent set of ground motion attenuation relations including data from the 1994 Northridge earthquake, *Seism. Res. Lett.* **66**, p. 23 (abstract).
- Dolan, J.F., K. Sieh, T.K. Rockwell, R.S. Yeats, J. Shaw, J. Suppe, G.J. Huftile, and E.M. Gath (1995). Prospects for larger and more frequent earthquakes in the Los Angeles Metropolitan Region, California. *Science* **267**, 199-205.
- Heaton, T.H., J.F. Hall, D.J. Wald, and M.W. Halling (1995). Response of high-rise and base-isolated buildings to a hypothetical Mw 7.0 blind thrust earthquake, *Science* **267**, 206-211.
- Kawase, H., T. Satoh and S. Matsushima (1995). Aftershock measurements and a preliminary analysis of aftershock records in Higashi-Nada Ward in Kobe after the 1995 Hyogo-Ken-Nambu earthquake, ORI Report 94-04.
- Kawase, H. and Y. Hayashi (1995). Strong motion simulation in Chuo Ward, Kobe, during the Hyogo-ken Nambu earthquake of 1995 based on the inverted bedrock motion, Architectural Institute of Japan
- Sekiguchi, H., K. Irikura, T. Iwata, Y. Kakechi, and M. Hoshiba (1995). Minute location of fault planes and source process of the 1995 Hyogo-Ken Nambu (Kobe), Japan earthquake from the waveform inversion of strong ground motion. *EOS* **76**, p. F378 (abstract).
- Somerville, P.G. and R.W. Graves (1993). Conditions that give rise to unusually large long period ground motions, *The structural design of tall buildings* **2**, 211-232.
- Somerville, P.G. and R.W. Graves (1995). Ground motion potential of the Los Angeles Region. *Proceedings of the 1995 Annual Meeting of the Los Angeles Tall Buildings Structural Design Council*, May 5.
- Somerville, P.G., N.F. Smith, R.W. Graves, and N.A. Abrahamson (1995). Representation of near-fault rupture directivity effects in design ground motions, and application to Caltrans bridges. *Proceedings of the National Seismic Conference on Bridges and Highways*, San Diego, December 10-13, 1995.

- Wald, D.J. and T.H. Heaton (1994). A dislocation model of the 1994 Northridge, California earthquake determined from strong ground motions, U.S. Geological Survey Open File Report 94-278.
- Wald, D.J. (1995). A preliminary dislocation model for the 1995 Kobe (Hyogo-ken nanbu), Japan, earthquake determined from strong motion and teleseismic waveforms, *Seism. Res. Lett.* 66, 22-28.
- Yoshida, S., K. Koketsu, B. Shibazaki, T. Sagiya, T. Kato, and Y. Yoshida (1995). Joint inversion of near- and far-field waveforms and geodetic data for the rupture process of the 1995 Kobe earthquake, manuscript submitted to *Journal of Physics of the Earth*.

17 January 1995 Hyogoken Nanbu Earthquake,  $M = 6.9$

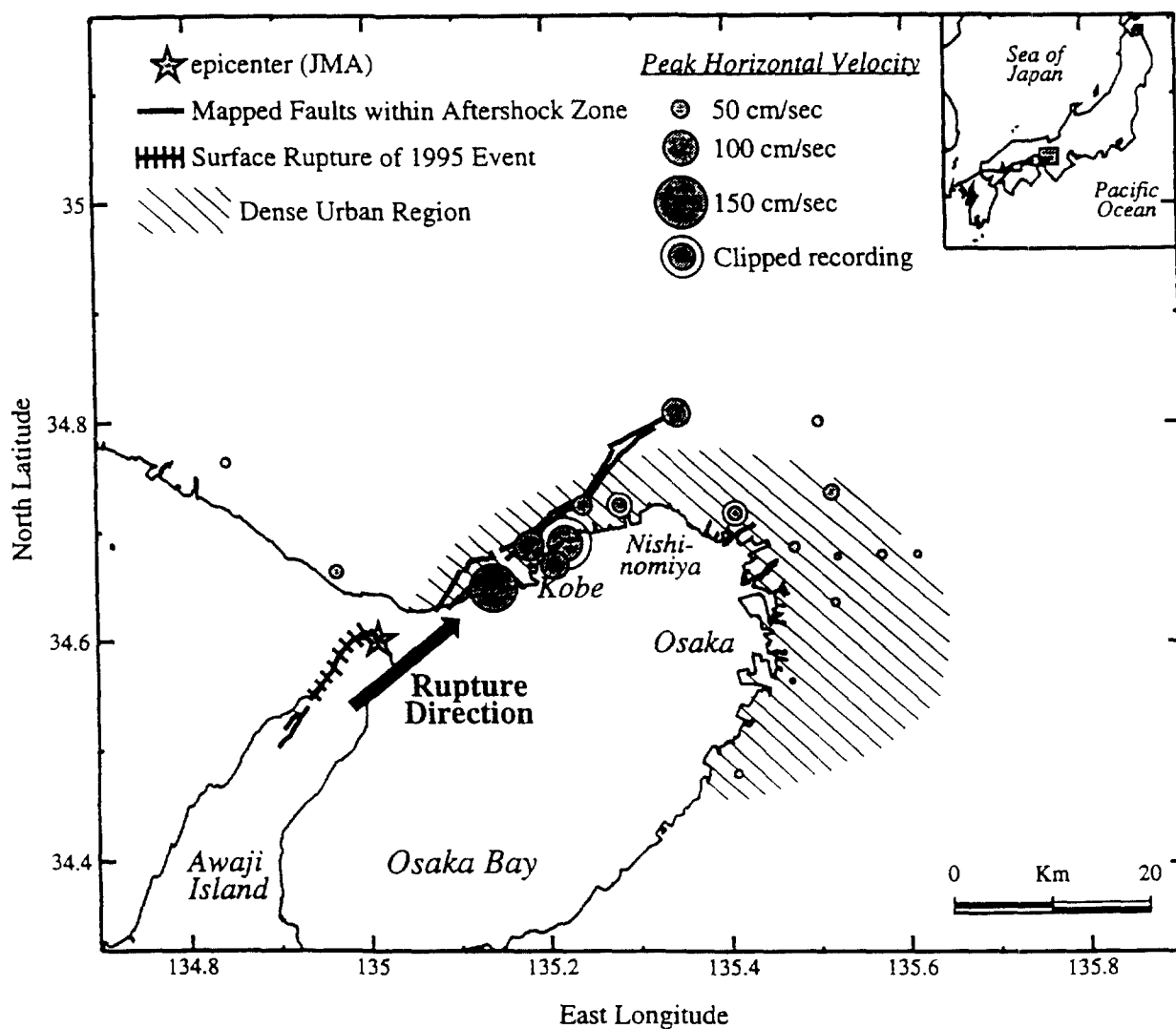


Figure 1. Location of the mainshock epicenter, mapped active faults within the aftershock zone (including surface rupture of the Nojima fault on Awaji Island), the dense urban region, and average horizontal peak velocities recorded from the 1995 Kobe earthquake.

# 17 Jan 95 Kobe, M6.9 - Kobe (JMA)

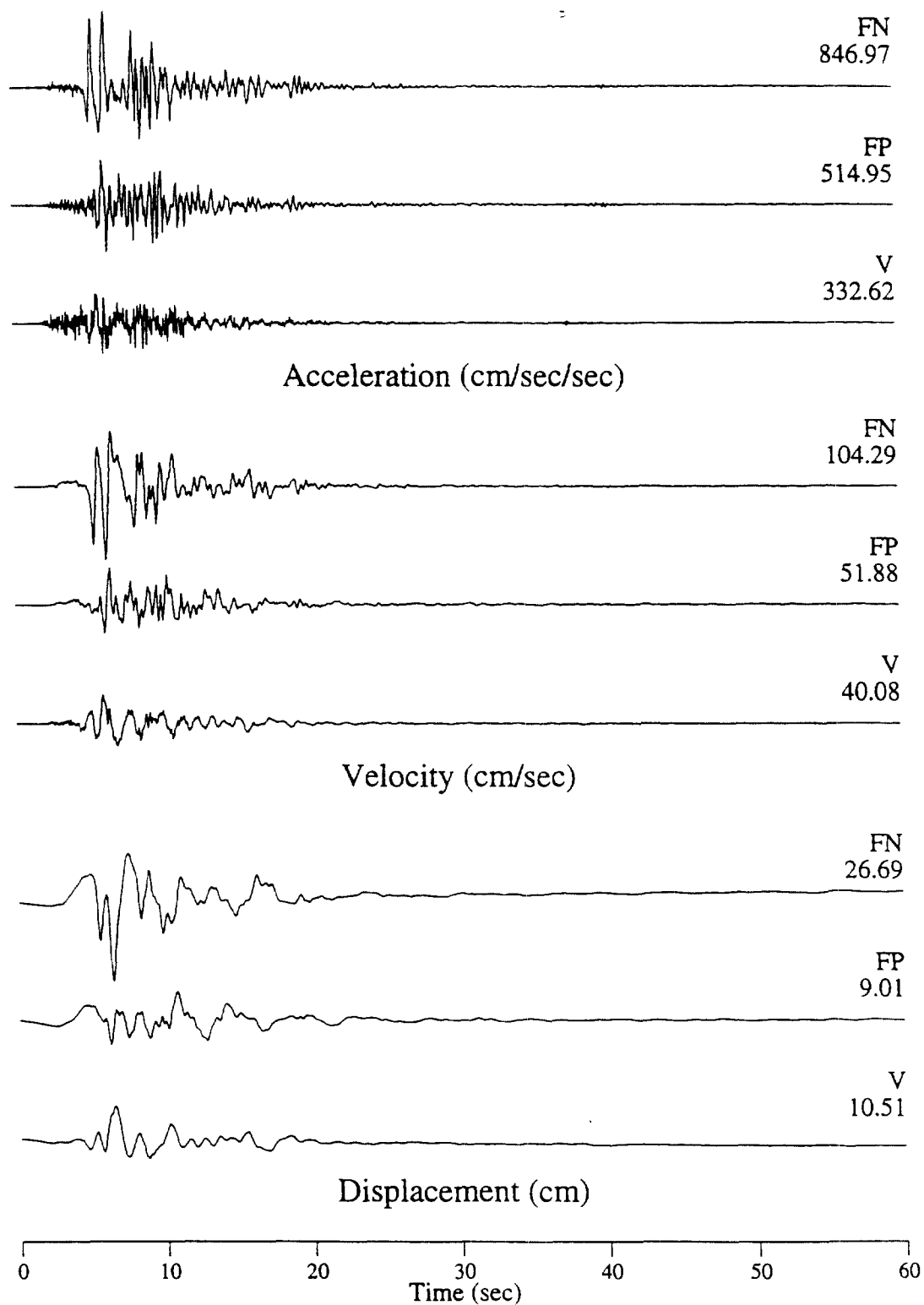


Figure 2. Recorded acceleration, velocity and displacement time histories of the 1995 Kobe earthquake at Kobe JMA rotated into fault-normal and fault-parallel components.

17 January 1995 Hyogoken Nanbu Earthquake, M=6.9

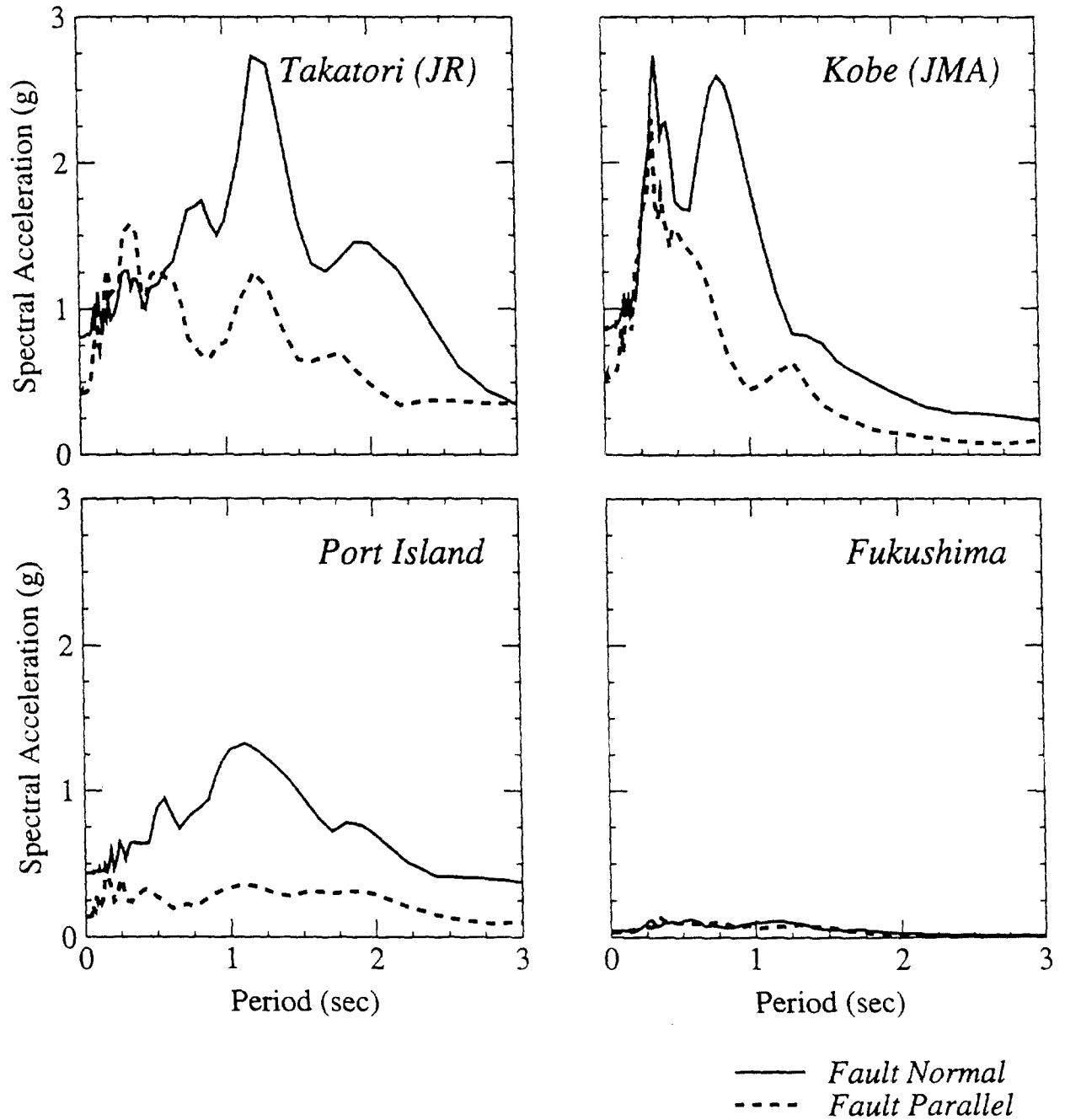


Figure 3. Response spectral acceleration of the fault-normal and fault-parallel components of the 1995 Kobe earthquake recorded at Takatori, Kobe JMA, and Port Island (forward directivity) and Fukushima (neutral directivity).

# 17 January 1994 Northridge Earthquake, $M=6.7$

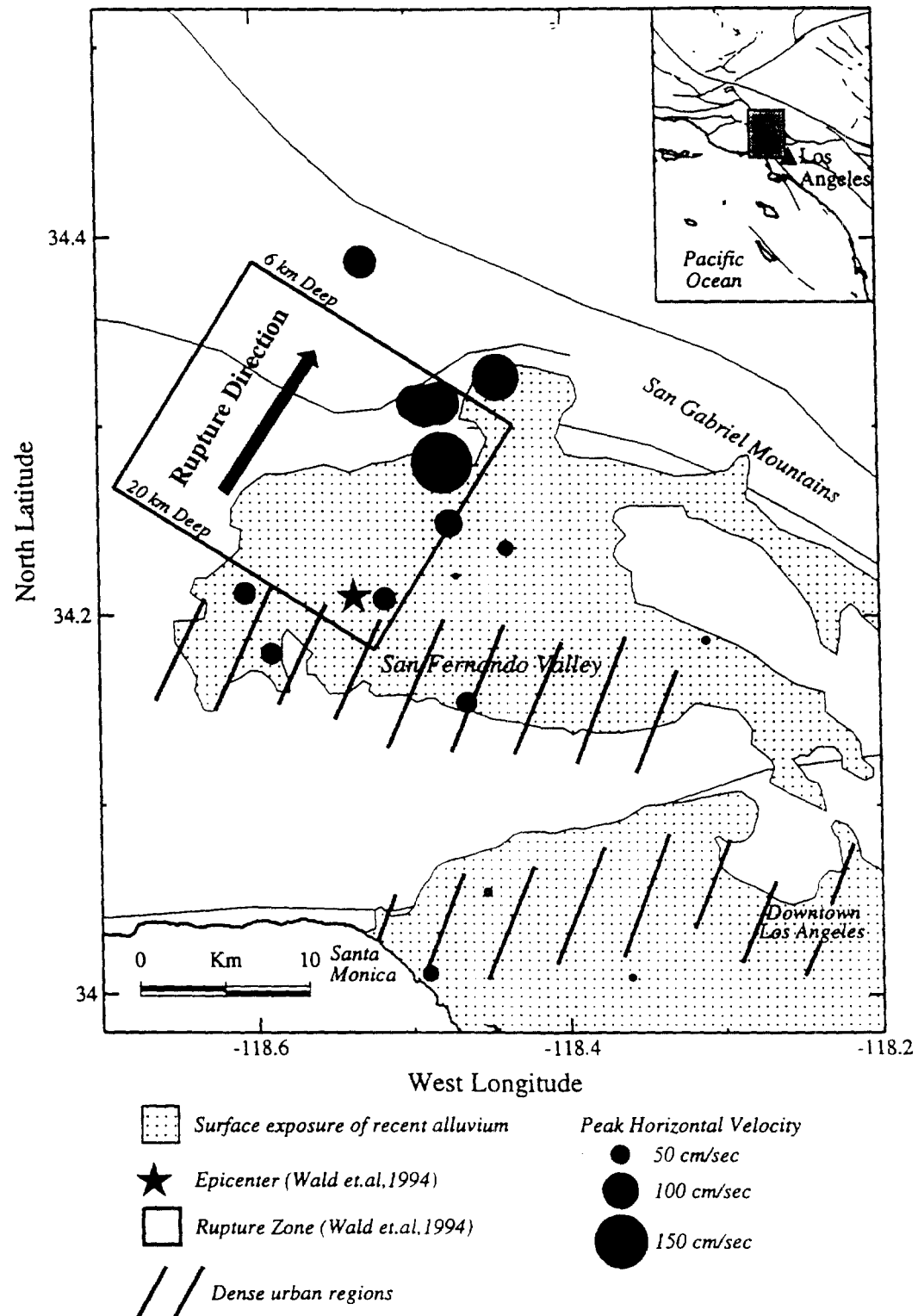


Figure 4. Location of the mainshock epicenter, surface projection of the fault rupture model of Wald and Heaton (1994), dense urban regions, and average horizontal peak ground velocities recorded from the 1994 Northridge earthquake.